



HAL
open science

Bis(N -cyclopropenio)-imidazol-2-ylidene: An N -Heterocyclic Carbene Bearing Two N -Cationic Substituents

Ajay Padunnappattu, Carine Duhayon, Vincent César, Yves Canac

► **To cite this version:**

Ajay Padunnappattu, Carine Duhayon, Vincent César, Yves Canac. Bis(N -cyclopropenio)-imidazol-2-ylidene: An N -Heterocyclic Carbene Bearing Two N -Cationic Substituents. *Organometallics*, 2022, 41 (20), pp.2868-2878. 10.1021/acs.organomet.2c00429 . hal-03818692

HAL Id: hal-03818692

<https://hal.science/hal-03818692>

Submitted on 18 Oct 2022

HAL is a multi-disciplinary open access archive for the deposit and dissemination of scientific research documents, whether they are published or not. The documents may come from teaching and research institutions in France or abroad, or from public or private research centers.

L'archive ouverte pluridisciplinaire **HAL**, est destinée au dépôt et à la diffusion de documents scientifiques de niveau recherche, publiés ou non, émanant des établissements d'enseignement et de recherche français ou étrangers, des laboratoires publics ou privés.

Bis(N-cyclopropenio)-imidazol-2-ylidene: An N-Heterocyclic carbene bearing two N-cationic substituents

Ajay Padunnappattu,[†] Carine Duhayon,[†] Vincent César^{*,†} and Yves Canac^{*,†}

LCC-CNRS, Université de Toulouse, CNRS, 205 route de Narbonne 31077 Toulouse cedex 4, France.

ABSTRACT: Thanks to the onio-substitution strategy, the tricationic imidazolium salt $(\mathbf{1}\cdot\text{H})(\text{OTf})_3$ featuring two N-cyclopropenio substituents was readily prepared in a two-step procedure from 1*H*-imidazole. The influence of the two cyclopropenium moieties on the electronic properties of the related dicationic NHC $\mathbf{1}^{2+}$ was evaluated on the basis of the $^1J_{\text{CH}}$, $\delta^{77}\text{Se}$, and TEP values obtained respectively from NHC precursor $(\mathbf{1}\cdot\text{H})(\text{OTf})_3$, NHC=Se adduct $(\mathbf{5})(\text{OTf})_2$, and NHC Rh(CO)₂ complex $(\mathbf{7})(\text{OTf})_2$, leading to the conclusion that carbene $\mathbf{1}^{2+}$ is one of the least-donating cationic NHCs reported to date. The coordinating ability of $\mathbf{1}^{2+}$ was extended to Pd(II) and Au(I) centers providing the dicationic $[\text{PdCl}(\text{allyl})(\mathbf{1})](\text{OTf})_2$ $(\mathbf{8})(\text{OTf})_2$, and $[\text{AuCl}(\mathbf{1})](\text{OTf})_2$ $(\mathbf{10})(\text{OTf})_2$ complexes which were fully characterized. While Pd complex $(\mathbf{8})(\text{OTf})_2$ was found to exhibit lability of a cyclopropenium substituent upon cleavage of a C⁺-N bond, Au complex $(\mathbf{10})(\text{OTf})_2$ was implemented in model Au-catalyzed intramolecular cyclization reactions showing moderate activity.

INTRODUCTION

While the design of electron-rich ligands of transition metals has been widely considered, mainly but not exclusively for catalytic applications,¹ that of their electron-poor counterparts has received much less attention and had relied mainly on the introduction of electron-withdrawing groups near the coordinating center.² Alternatively, locating a positive charge in close proximity to this center has been shown to constitute a powerful strategy to make the metal more electro-deficient. This specific scenario was achieved in P-based ligands with imidazolio- A^+ and cyclopropeniophosphines B^+ , both representatives of the carbeniophosphine (also called α -cationic phosphines) class,³ where a stabilized carbenium center, brought by an imidazolium^{3a} or a cyclopropenium^{3b} moiety respectively, is directly bonded to the coordinating P(III) atom (Figure 1).

Following this, the Lewis base character of the P-center was further lowered by the introduction of a second cationic P-substituent as demonstrated with the report of diimidazolio- A^{2+} ,⁴ and dicyclopropeniophosphines B^{2+} .⁵ A similar strategy was applied with C(II)-centered ligands, especially in the case of N-Heterocyclic carbenes (NHCs) widely known today for their predominant role in organometallic chemistry, homogeneous catalysis, and functional materials.⁶ Different approaches for the synthesis of cationic NHCs were thus considered depending of the nature of the fragment bearing the positive charge, the position of the charge relative to the NHC, and the nature of the connection between them.⁷ Keeping a close proximity between the charge and the sp^2 hybridized carbene atom in order to have a significant impact on the stereoelectronic properties of the coordinating center, three main families of such cationic species were reported, the charge being either included in the π -system of the NHC,⁸ or covalently bonded to a C-⁹ or a N-atom¹⁰ of the carbene backbone. In this specific field, we have recently prepared the cationic NHC C^+ , belonging to the last category,

featuring a N-bounded 2,3-bis(diisopropylamino)cyclopropenium group and proved its ability to coordinate Pd(II), Rh(I), and Au(I) metal centers (Figure 1).¹¹ The inductive withdrawing effect of the cyclopropenium ring was found to lower the σ -donation and to exalt the π -acidity of the carbene relative to the neutral IMes prototype while maintaining significant catalytic activity in intramolecular Au(I)-induced cyclizations.

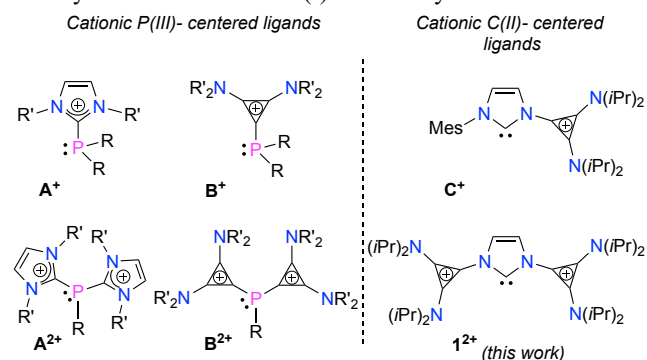
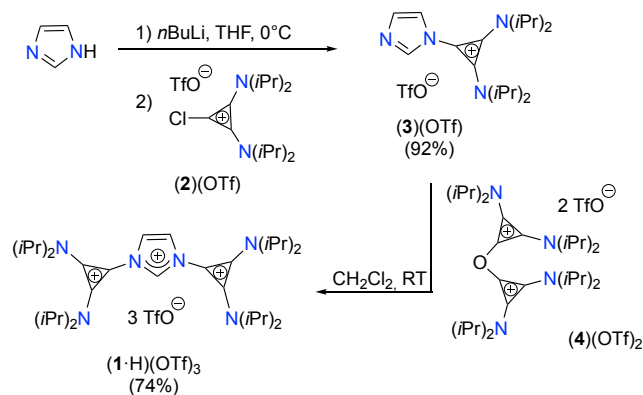


Figure 1. Analogy between mono- ($\text{A}^+ - \text{B}^+$)³ and dicationic phosphines ($\text{A}^{2+} - \text{B}^{2+}$)^{4,5} (left) vs mono- (C^+)¹¹ and dicationic NHCs $\mathbf{1}^{2+}$ (right).

By analogy with the α -dicationic phosphine series,^{4,5} the present contribution addresses the preparation of the dicationic NHC $\mathbf{1}^{2+}$ resulting from the introduction of a second N-bis(diisopropylamino)cyclopropenio substituent. Thus, the main objectives of this work are to evaluate the influence of the presence of two positive charges on the stereoelectronic properties and coordinating ability of the carbene center, as well as to study the catalytic efficiency of ensuing metal complexes.

RESULTS AND DISCUSSION

The targeted tricationic imidazolium salt $(1\cdot\text{H})(\text{OTf})_3$ was synthesized in a two-step sequence from readily available 1*H*-imidazole. In a first step, the *N*-cyclopropenium imidazole $(3)(\text{OTf})$ was isolated in 92% yield by reacting 1*H*-imidazole with one equivalent of *n*BuLi in THF at 0°C followed by the addition of 1-chlorocyclopropenium triflate $(2)(\text{OTf})$.¹² Then, in a second time as no reaction was observed by treating imidazole $(3)(\text{OTf})$ with another equiv. of $(2)(\text{OTf})$ even in the presence of a chloride scavenger (NaOTf or Me₃SiOTf), based on the elegant onio-substitution strategy,¹³ the more reactive dicationic cyclopropenium derivative $(4)(\text{OTf})_2$ was added to imidazole $(3)(\text{OTf})$ in CH₂Cl₂ at RT. Under these mild conditions, we were pleased to observe the formation of the pre-ligand $(1\cdot\text{H})(\text{OTf})_3$ isolated in 74% yield as a white microcrystalline solid (Scheme 1).



Scheme 1. Synthesis of the tricationic salt $(1\cdot\text{H})(\text{OTf})_3$ from 1*H*-imidazole and 1-chlorocyclopropenium triflate $(2)(\text{OTf})$.

The formation of salt $(1\cdot\text{H})(\text{OTf})_3$ was clearly evidenced by the presence of the characteristic low field ¹H NMR signal of the imidazolium proton at δ_{H} 10.8 ppm compared to that of the imidazole precursor $(3)(\text{OTf})$ (δ_{H} 7.9 ppm). The exact structures of cationic salts $(3)(\text{OTf})$ and $(1\cdot\text{H})(\text{OTf})_3$ were unambiguously confirmed by X-ray diffraction analysis of single crystals.¹⁵ Concerning $(1\cdot\text{H})(\text{OTf})_3$, the main information concerns the existence of a plane of symmetry orthogonal to the imidazolium ring and intersecting it along the C1–H1 bond (Figure 2). The cyclopropenium and imidazolium rings are almost orthogonal to each other with a dihedral angle C1–N1–C3–C5 value of 93.76° (Figure 2). As observed in the related mono(*N*-cyclopropenium) imidazolium salt $(\text{C}\cdot\text{H})(\text{OTf})_2$ recently described,¹¹ all the *N*-atoms of cationic substituents are *sp*² hybridized and coplanar with the cyclopropenyl rings due to the strong interaction of the *N*-lone pairs with the two π -electron aromatic system. The rather long C3–N1 bond distance [1.405(5) Å] indicates a weak interaction between the cationic *N*-substituents and the central imidazolium ring. It's worth mentioning that $(1\cdot\text{H})(\text{OTf})_3$ can be formally described as an electrostatic pincer with the presence of a triflate anion intercalated between the two cyclopropenium moieties (C⁺...O ~ 3.38 Å). This specific positioning certainly contributes to the overall stabilization of the edifice in the crystalline state and is probably partly responsible for the perfect symmetry of the molecule.

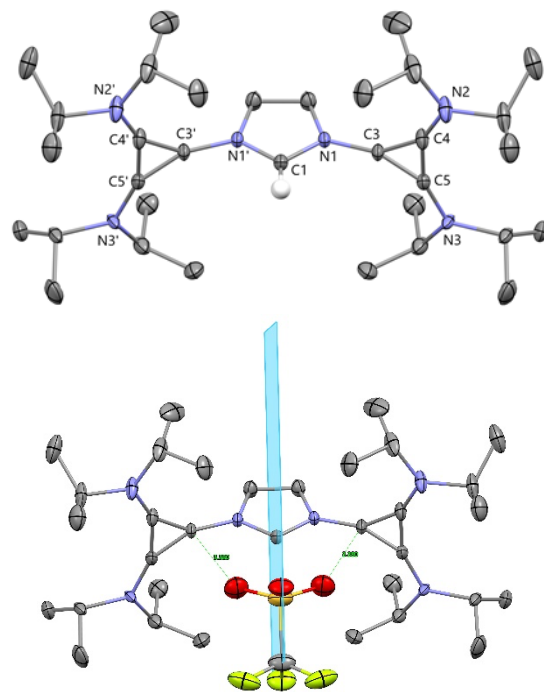
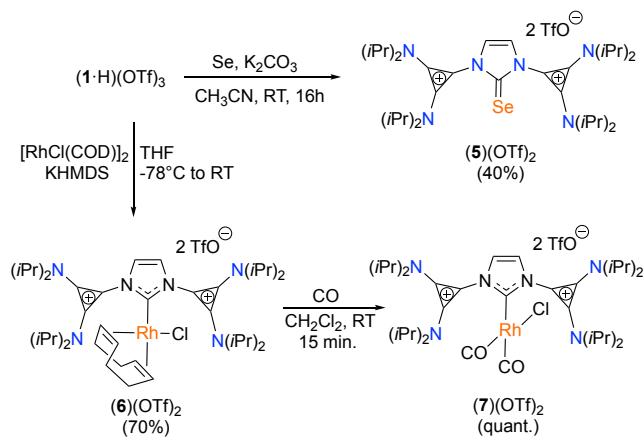


Figure 2. Perspective views of the cationic part of imidazolium salt $(1\cdot\text{H})(\text{OTf})_3$ (top) with thermal ellipsoids drawn at the 30% probability level. The H atoms and OTf anions are omitted for clarity. Representation of the mirror plane with intercalated OTf anion in $(1\cdot\text{H})(\text{OTf})_3$ (bottom). Selected bond lengths (Å) and bond angles (°). $(1\cdot\text{H})(\text{OTf})_3$: C1–N1 = 1.331(5); C3–N1 = 1.405(5); C3–C4 = 1.362(6); C3–C5 = 1.357(6); C4–C5 = 1.425(6); N1–C1–N1 = 107.3(6); C1–N1–C3 = 124.0(4); N1–C3–C4 = 147.6(4); C4–C3–C5 = 63.2(3).

To evaluate the influence of the two cyclopropenium substituents on the stereoelectronic properties of NHC $\mathbf{1}^{2+}$,¹⁶ we turned first our attention to the ¹J_{CH} coupling constant between the pre-carbenic carbon atom and the connected hydrogen in the imidazolium precursor $(1\cdot\text{H})(\text{OTf})_3$.¹⁷ The value of ¹J_{CH} = 232 Hz superior to that of mono(*N*-cyclopropenium) imidazolium salt $(\text{C}\cdot\text{H})^{2+}$ (¹J_{CH} = 229 Hz) indicates that the introduction of a second positive charge lowers further the σ -donation of the carbene center. Of note, the ¹J_{CH} values of imidazolium salts based on neutral IMes and IMes^{Cl2} of 225 and 232 Hz,¹⁸ and of other related dicationic NHC precursors $(\text{E}\cdot\text{H})^{2+}$,^{9b} $(\text{F}\cdot\text{H})^{2+}$,^{10b} and $(\text{G}\cdot\text{H})^{2+}$,^{8c} of 231, 224, and 227 Hz, revealing that $\mathbf{1}^{2+}$ is one of the least σ -donating NHCs known to date (Table 1). To assess the π -acidity of carbene $\mathbf{1}^{2+}$,¹⁹ the selenourea $(5)(\text{OTf})_2$ was prepared by reacting the pre-ligand $(1\cdot\text{H})(\text{OTf})_3$ with an excess of selenium in the presence of K₂CO₃ in MeCN at RT (Scheme 2).²⁰ The NHC=Se adduct $(5)(\text{OTf})_2$ isolated in 40% yield was fully characterized including by an X-ray diffraction analysis (Figure 3, Table 2).¹⁵ Compared to NHC=Se adduct of C⁺ (δ_{Se} = 112 ppm),¹¹ the ⁷⁷Se chemical shift of $(5)(\text{OTf})_2$ (δ_{Se} = 197 ppm) is strongly downfield shifted, and only carbenes **D**⁺ and **G**⁺ (δ_{Se} = 245 and 473 ppm)^{8a,8c} where the positive charge is delocalized through the π -system of the *N*-heterocycle present more π -acidic character (Table 1). The ¹J_{CH} and δ_{Se} values reveal thus that the introduction of a second cationic *N*-substituent significantly influences both the σ -donation and the π -accepting characters of carbene $\mathbf{1}^{2+}$.

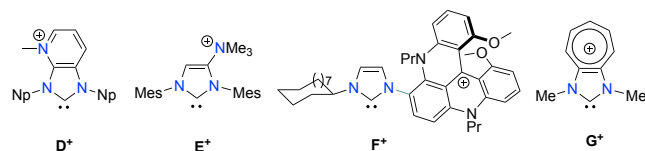


Scheme 2. Synthesis of the selenourea **(5)(OTf)₂** and NHC Rh(I) complexes **(6)(OTf)₂** and **(7)(OTf)₂** from **(1-H)(OTf)₃**.

Table 1. Electronic parameters of selected imidazol-2-ylidenes.

NHC	¹ J _{CH} (Hz) ^[a]	δ ⁷⁷ Se (ppm) ^[b]	TEP (cm ⁻¹) ^[c]
IMes	225	27	2051
IMes ^{Cl2}	232	114	2055
C ⁺ ^[d]	229	112	2057
D ⁺ ^[e]	-	245	2067
E ⁺ ^[f]	231	102	2056
F ⁺ ^[g]	224	65, 49	2055
G ⁺ ^[h]	227	473	2070
1²⁺	232	197	2061

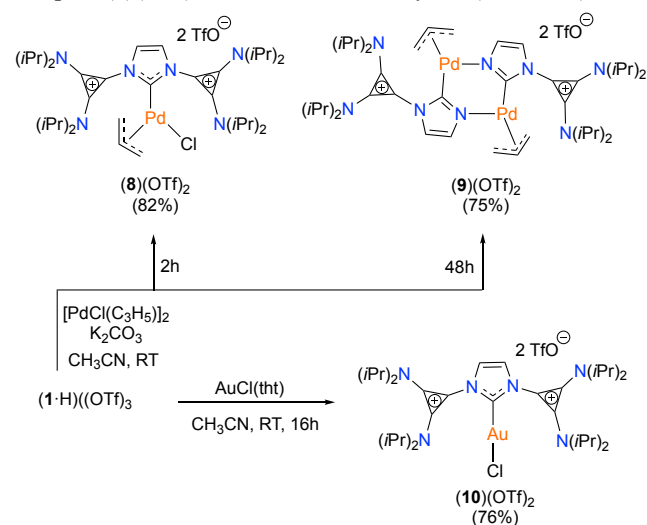
[a] Measured on (NHC·H)⁺ precursors. [b] Measured on NHC=Se adducts. [c] Determined from NHC-Rh(CO)₂ complexes. [d] From reference 11. [e] From reference 8a. [f] From reference 9b. [g] From reference 10b. [h] From reference 8e.



The overall electronic donation of NHC **1²⁺** was then estimated by the preparation of the corresponding Rh(CO)₂ complex. To this purpose, the salt **(1-H)(OTf)₃** was first treated with 0.5 equiv. of [RhCl(COD)]₂ in the presence of KHMDS in THF at -78°C (Scheme 2). The corresponding NHC Rh(I) complex **(6)(OTf)₂** was isolated in 70% yield showing that, despite some weak donating character, carbene **1²⁺** retains sufficient coordinating ability to form stable metal complexes. Interestingly, although with slightly lower yield (ca. 60%), complex **(6)(OTf)₂** could be also isolated from **(1-H)(OTf)₃** under similar “weak-base” conditions ([RhCl(COD)]₂, K₂CO₃, MeCN, RT) already used for the formation of NHC=Se adduct **(5)(OTf)₂**. Finally, bubbling CO for 15 min through a CH₂Cl₂ solution of **(6)(OTf)₂** at RT afforded quantitatively the targeted NHC Rh(CO)₂ complex **(7)(OTf)₂**. Although the latter was not isolated, ¹³C NMR spectroscopy evidenced the presence of the two characteristic CO signals with appropriate multiplicity at δ_c 183.5 ppm (d, J_{CRh} = 55.0 Hz) and δ_c 181.9 ppm (d, J_{CRh} = 72.1 Hz). The IR CO stretching frequencies of **(7)(OTf)₂** were measured at 2007

and 2094 cm⁻¹ in CH₂Cl₂. The calculated Tolman Electronic Parameter (TEP)²¹ value for NHC **1²⁺** of 2061 cm⁻¹ indicates that only planar cationic carbenes **D⁺** and **G⁺** are characterized by a weaker overall donating character,²² and that the substitution of the neutral mesityl groups in IMes by the cationic cyclopropenium substituent diminishes sequentially the overall electronic donation of the corresponding NHC (IMes: 2051 vs **C⁺**: 2057 vs **1²⁺**: 2061 cm⁻¹).

Being able to stabilize Rh(I) centers, we next investigated the possibility of NHC **1²⁺** to coordinate other transition metals. In the Pd(II) series, the direct and mild treatment of **(1-H)(OTf)₃** with half an equiv. of [PdCl(π-allyl)]₂ in the presence of an excess of K₂CO₃ in MeCN at RT produced cleanly the NHC Pd(allyl)Cl complex **(8)(OTf)₂** in 82% yield (Scheme 3). Unexpectedly, under similar experimental conditions but with a longer reaction time – approximately 48h – the dimeric NHC Pd(II) complex **(9)(OTf)₂** was isolated in 75% yield (Scheme 3).



Scheme 3. Preparation of metal NHC complexes **(8)(OTf)₂**, **(9)(OTf)₂**, and **(10)(OTf)₂** from imidazolium salt **(1-H)(OTf)₃**.

Both cationic Pd complexes were fully characterized, including by X-ray diffraction analysis (Figure 3, Table 2).¹⁵ In **(8)(OTf)₂**, the Pd(II) atom resides in a classical square-planar environment where the coordination plane defined by the Cl, C1, C11 atoms and allyl fragment is deviated with respect to the NHC ring (dihedral angle N1–C1–Pd1–C11: 34.13°). Due to the coordination sphere of the Pd center, there is no crystallographic mirror and the two cyclopropenium substituents are almost orthogonal to the carbenic ring with different dihedral angles (C1–N2–C4–C6: 94.42° and C1–N1–C7–C9: 80.22°). Noteworthy the chloride co-ligand is oriented towards one of the cyclopropenium moieties (C⁺...Cl ~ 3.21 Å). Regarding **(9)(OTf)₂**, the XRD analysis revealed a totally different picture, the complex being dimeric in nature based on a central six-membered boat-shaped dipallacycle where each Pd(II) atom in a square-planar environment is surrounded by the C1 atom of an imidazolyl ligand, the sp² hybridized N-atom of another imidazolyl fragment and a π-allyl co-ligand. In this complex, each imidazolyl moiety acts formally as an anionic L,X-type bridging ligand.

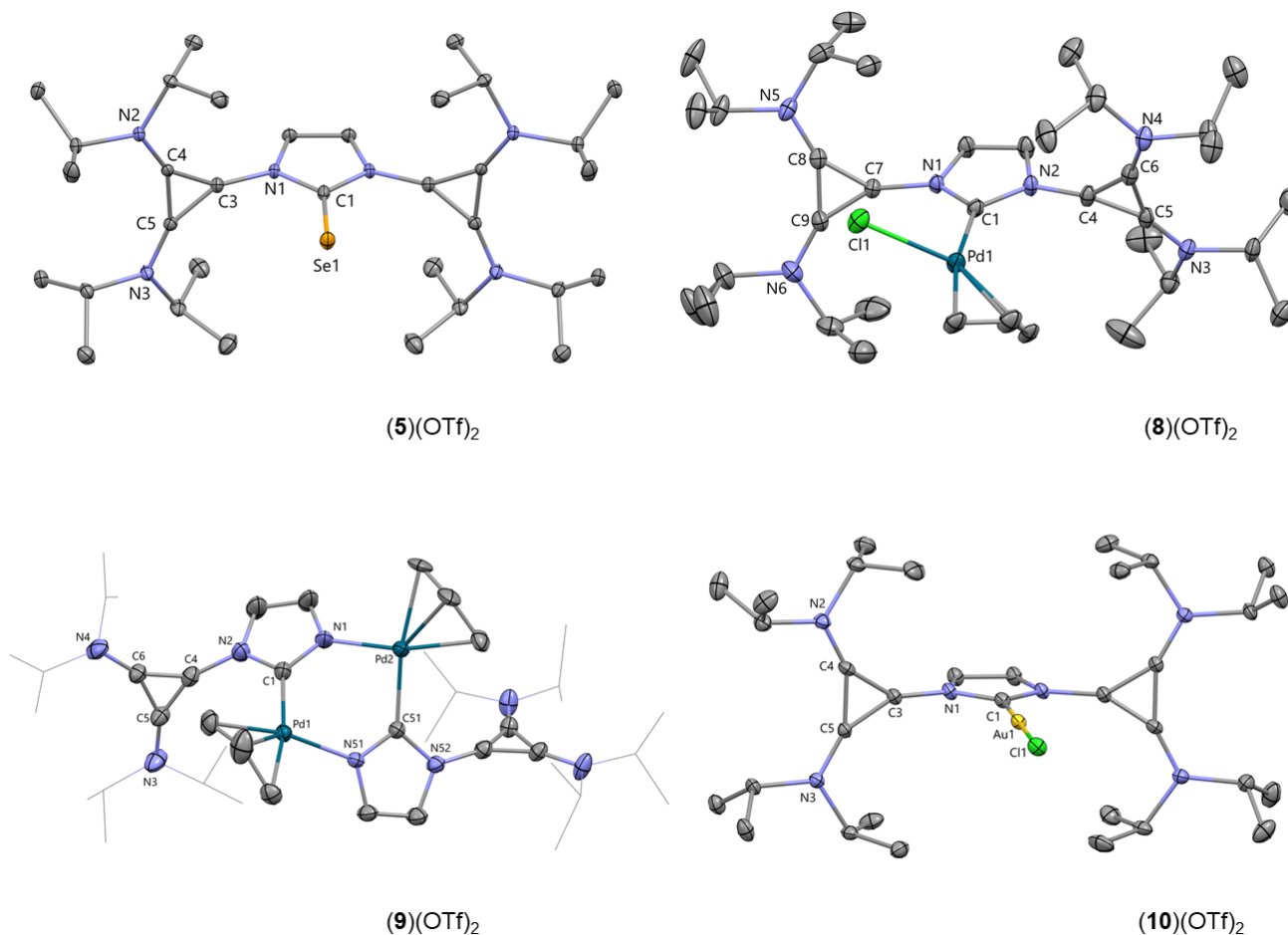
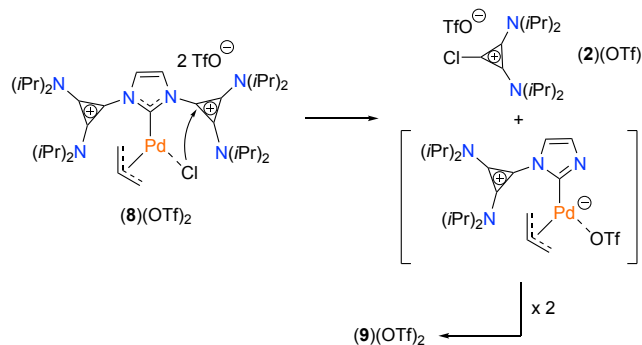


Figure 3. Perspective views of the cationic part of NHC=Se adduct **(5)(OTf)₂**, NHC Pd(II) **(8)(OTf)₂**, **(9)(OTf)₂**, and Au(I) **(10)(OTf)₂** complexes with thermal ellipsoids drawn at the 30% probability level. The H atoms and OTf anions are omitted for clarity.

Table 2. Selected bond lengths (Å) and bond angles (°) for **(5)(OTf)₂**, **(8)(OTf)₂**, **(9)(OTf)₂**, and **(10)(OTf)₂**.

(5)(OTf)₂	(8)(OTf)₂	(9)(OTf)₂	(10)(OTf)₂
C1–Se1: 1.825(4)	C1–Pd1: 2.056(4)	C1–Pd1: 2.031(6)	C1–Au1: 1.982(4)
C1–N1: 1.363(3)	C1–N1: 1.365(5)	N1–Pd2: 2.119(6)	C1–N1: 1.346(3)
N1–C3: 1.393(3)	C1–N2: 1.360(5)	C1–N1: 1.334(8)	N1–C3: 1.405(3)
C3–C4: 1.368(4)	N1–C7: 1.398(4)	C1–N2: 1.379(8)	C3–C4: 1.367(3)
C3–C5: 1.367(4)	N2–C4: 1.413(5)	N2–C4: 1.407(8)	C3–C5: 1.364(3)
C4–C5: 1.434(4)	Pd1–Cl1: 2.3823(10)	C4–C5: 1.335(9)	C4–C5: 1.445(3)
N1–C1–N1: 104.1(3)	N1–C1–N2: 102.1(3)	C4–C6: 1.354(8)	Au1–Cl1: 2.2820(9)
N1–C1–Se1: 127.97(16)	N1–C1–Pd1: 129.0(3)	C5–C6: 1.419(8)	N1–C1–N1: 103.9(3)
C1–N1–C3: 122.8(2)	C1–Pd1–Cl1: 99.22(10)	N1–C1–N2: 105.8(5)	N1–C1–Au1: 128.05(15)
N1–C3–C4: 148.8(3)	C1–N1–C7: 125.6(3)	N1–C1–Pd1: 125.4(5)	C1–Au1–Cl1: 179.994
N1–C3–C5: 147.9(2)	C1–N2–C4: 125.8(3)	C1–N2–C4: 124.2(5)	C1–N1–C3: 125.0(2)
C4–C3–C5: 63.24(19)	N1–C7–C8: 146.4(4)	C1–N1–Pd2: 123.7(5)	N1–C3–C4: 147.6(2)

To our knowledge this type of dinuclear structure is unique and more generally imidazolyl complexes are highly reactive and therefore rarely isolated.²³ A plausible mechanism would imply the nucleophilic attack of a decoordinated chloride anion at the neighboring electrodeficient carbon atom of a N-cyclopropenium substituent resulting in the elimination of 1-chlorocyclopropenium triflate (**2**)(OTf) with formation of an imidazolyl Pd intermediate which would stabilize by dimerization to give the Pd complex (**9**)(OTf)₂ experimentally observed (Scheme 4).²⁴ A concerted intramolecular mechanism without chloride dissociation cannot be excluded, as well as residual traces of H₂O which in the presence of K₂CO₃ base could play a similar role to that of the chloride anion in the formation of dimer (**9**)(OTf)₂.



Scheme 4. Possible mechanism for the formation of NHC Pd dimer (**9**)(OTf)₂ from (**8**)(OTf)₂ upon cleavage of a N-C⁺ bond promoted by chloride anion.

After the coordination of Rh(I) and Pd(II) centers, we decided to explore the coordination chemistry of NHC **1**²⁺ towards Au(I) metal precursors. According to the conditions developed previously, the pre-ligand (**1.H**)(OTf)₃ was reacted with AuCl(tht) using K₂CO₃ as a base in MeCN at RT. The corresponding dicationic NHC AuCl complex (**10**)(OTf)₂ was thus isolated as a pale yellow solid in 76% yield (Scheme 3) whose molecular structure was determined by an X-ray diffraction analysis of monocrystals obtained in a CH₂Cl₂/Et₂O mixture (Figure 3, Table 2).¹⁵ As expected, Au(I) complex (**10**)(OTf)₂ presents a typical linear geometry (Cl–Au1–Cl1: 179.994°) that accommodates the existence of plane of symmetry as observed in the pre-ligand (**1.H**)(OTf)₃ and NHC=Se adduct (**5**)(OTf)₂.

From Au complex (**10**)(OTf)₂, the steric constraint induced by the dicationic NHC ligand **1**²⁺ was calculated using the SambVca web application.²⁵ The carbene **1**²⁺ was found to provide a steric pressure in between the smaller mono-cationic NHC **C**⁺ and the bigger neutral IPr NHC (Figure 4). More precisely, the two cyclopropenium groups induce equal steric pressure in all quadrants with %V_{bur} = 39.7% which can be related to the perfect symmetry of the NHC ligand observed in Au complex (**10**)(OTf)₂ [%V_{bur}(IMes) = 36.5%; %V_{bur}(C) = 38.2%; %V_{bur}(IPr) = 45.7%]. In the same series of complexes, another valuable information concerns the reduction potentials (E_p^{Red}) considering that such values generally reflect the electronic properties of the ligands. The different Au(I) complexes were thus investigated by cyclic voltammetry showing that all the reductions are irreversible with E_p^{Red} values varying according to the electron-donating nature of the NHC ligand. Indeed, due to the electron-withdrawing character of cyclopropenium group, dicationic complex (**10**)(OTf)₂ exhibits higher reduction

potential at E_p^{Red} = -1.66 V vs SCE compared to mono-cationic (C)AuCl (E_p^{Red} = -1.84 V vs SCE) and neutral (IMes)AuCl (E_p^{Red} = -2.25 V vs SCE) complexes.

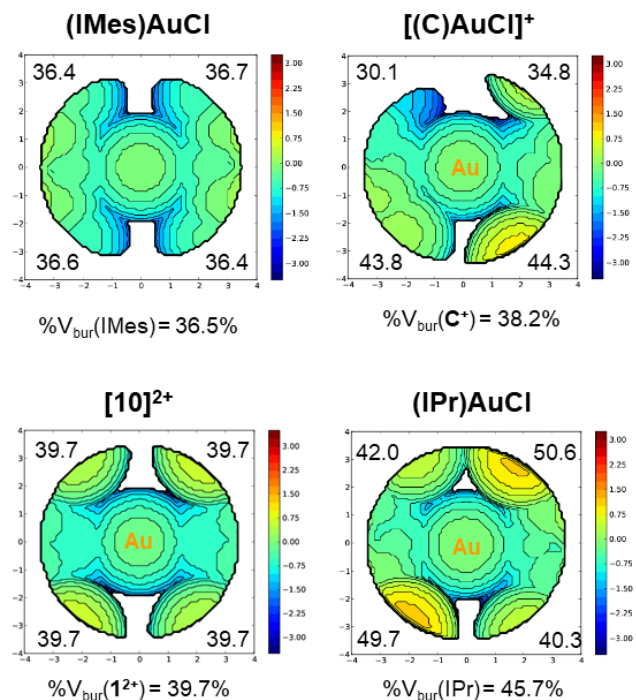
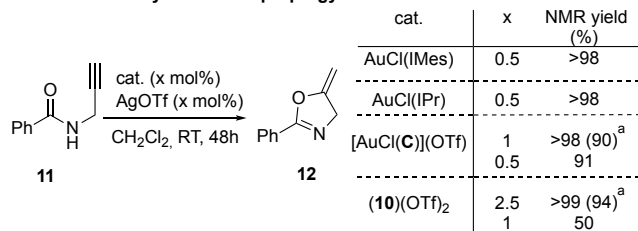


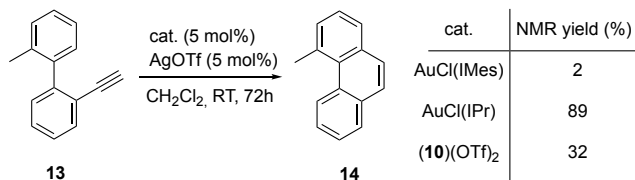
Figure 4. Comparative steric maps of (IMes)AuCl, (C)AuCl, (**10**)(OTf)₂, and (IPr)AuCl complexes. Values given in the four corners of the map are the %V_{bur} of the ligands in the corresponding quadrant.

To investigate the activity of dicationic gold complex (**10**)(OTf)₂ in homogeneous catalysis, the intramolecular cyclizations of propargyl amide **11** and of 2-ethynyl-2'-methyl-1,1'-biphenyl **13** were chosen as model reactions. Noteworthy, the Au-catalyzed cyclization of **11** had previously served as a standard catalytic reaction for cationic NHCs,^{10a,26} and that of **13** for α -dicationic phosphines (Scheme 5).^{5a} The pre-catalyst (**10**)(OTf)₂ was found to present catalytic activity leading to full conversion of propargyl amide **11** into the five-membered heterocycle **12** in 48 hours with a catalytic loading of 2.5 mol%. However, decreasing the catalytic loading to 1.0 mol% had a significant impact on activity, affording only a 50% NMR yield after 48 hours. The catalytic activity of complex (**10**)(OTf)₂ was then compared with that of neutral (IMes)AuCl and (IPr)AuCl, and mono-cationic [(C)AuCl](OTf) complexes (Scheme 5). As reported in the table, all Au(I) NHC complexes present higher efficiency than (**10**)(OTf)₂ which can be tentatively rationalized by the relative fragility of the ligand **1**²⁺, as demonstrated in the Pd(II) series with the formation of the dimeric complex (**9**)(OTf)₂ upon cleavage of a N-C⁺ bond. Interestingly, in the catalytic intramolecular cyclization of 2-ethynyl-2'-methyl-1,1'-biphenyl, the dicationic NHC complex (**10**)(OTf)₂ performs better than neutral (IMes)AuCl complex with 32% NMR yield after 72 hours and a catalytic loading of 5%. However, it remains less active than (IPr)AuCl complex certainly for the same reasons of stability mentioned above.

Intramolecular cyclization of propargyl amide



Intramolecular hydroarylation



Scheme 5. Comparative catalytic studies in Au(I)-catalyzed reactions. ^a isolated yield in parentheses.

CONCLUSION

In summary, we have synthesized and fully characterized five metal complexes of the new α,α' -dicationic NHC 1^{2+} bearing two 2,3-bis(diisopropylamino)cyclopropenyl substituents in the Rh(I) [(6)(OTf)₂, (7)(OTf)₂], Pd(II) [(8)(OTf)₂, (9)(OTf)₂] and Au(I) (10)(OTf)₂ series. Compared to the N-cyclopropenyl-imidazol-2-ylidene recently reported, according to ¹J_{CH} coupling constants, ⁷⁷Se chemical shifts, and TEP values of NHC precursors, NHC=Se adducts, and NHC Rh(CO)₂ complexes, the introduction of a second cationic N-substituent was shown to significantly influence the stereoelectronic properties of the carbene center, further contributing to decrease its σ -donation and increase its π -acidity. In the Pd case, a certain lability of a cyclopropenium fragment due to the cleavage of a N-C⁺ bond was evidenced affording the dimeric Pd(II) complex (9)(OTf)₂ of an anionic bidentate L,X-type imidazolyl ligand. This peculiar reactivity was proposed to rationalize the moderate catalytic activity of Au(I) complex (10)(OTf)₂ observed in the intramolecular cyclization of N-(2-propyn-1-yl)benzamide and 2-ethynyl-2'-methyl-1,1'-biphenyl. We strongly believe that this approach based on the onio-substitution strategy presents a high potential in the development of other cationic NHC platforms. However, it appears essential to develop more robust cationic NHCs, such as systems where the cationic substituents would be annelated laterally to the N-heterocycle. More generally, our future efforts will focus on the preparation of cationic ligands characterized by a stronger interaction between the charge and the coordination site for applications in the fields of catalysis and materials.

EXPERIMENTAL SECTION

General Remarks.

All manipulations were performed under an inert atmosphere of dry nitrogen by using standard vacuum line and Schlenk tube techniques. Glassware was dried at 120°C in an oven for at least three hours. THF, Et₂O, pentane, toluene and CH₂Cl₂ were dried using an Innovative Technology solvent purification system. Acetonitrile was dried using a MBraun SPS column. 2,3-bis(diisopropylamino)-1-chlorocyclopropenium triflate (2)(OTf),¹² (4)(OTf)₂,¹⁴ [PdCl(allyl)]₂,²⁷ and AuCl(tht),²⁸ were prepared according to literature procedures. All other reagents were commercially available and used as received. Chromatographic purification was carried out on silica gel (SiO₂, 63–200 μ m). Solution IR spectra were recorded in 0.1 mm CaF₂ cells using a Perkin Elmer Frontier FT-IR spectrometer and given in cm⁻¹. ¹H and

¹³C NMR spectra were obtained on Bruker AV300, AV400 or NEO600 spectrometers. NMR chemical shifts δ are in ppm, with positive values to high frequency relative to the tetramethylsilane reference for ¹H and ¹³C, and to pure Me₂Se in C₆D₆ for ⁷⁷Se. If necessary, additional information on the carbon signal attribution was obtained using ¹³C{¹H}, *J*-modulated spin-echo (JMOD) ¹³C{¹H}, ¹H-¹³C HMQC, and/or HMBC experiments. MS spectra (ESI mode) were performed by the mass spectrometry service of the "Institut de Chimie de Toulouse". Voltammetric measurements were performed by the electrochemistry service of the LCC with a potentiostat Autolab PGSTAT100 controlled by GPES 4.09 software. Experiments were performed at room temperature in a homemade airtight three-electrode cell consisting of a Pt working electrode (*d* = 0.5 mm), a platinum wire (*S* = 1 cm²) as counter electrode, and a saturated calomel electrode (SCE) separated from the solution by a bridge compartment as a reference. Before each measurement, the working electrode was cleaned with a polishing machine (Presi P230, P4000). The measurements were carried out in dry CH₂Cl₂ under argon atmosphere using 0.1 M [*n*Bu₄N](OTf) (Fluka, 99% puriss electrochemical grade) as supporting electrolyte and typically 10⁻³ M sample concentration.

1-(imidazol-1-yl)-2,3-bis(diisopropylamino)cyclopropenium triflate (3)(OTf). 1*H*-imidazole (226 mg, 3.32 mmol, 1 equiv) was placed in a Schlenk tube which was evacuated and backfilled with N₂. THF (10 mL) was added and the reaction mixture was stirred for 5 minutes for complete dissolution. The reaction mixture was then cooled to 0°C and *n*BuLi was added (1.6 M in hexane, 2.2 mL, 3.48 mmol, 1.05 equiv). The solution was warmed to room temperature. After 30 minutes the reaction was cooled to 0°C and 2,3-bis(diisopropylamino)-1-chlorocyclopropenium triflate (2)(OTf) (1.39 g, 3.32 mmol, 1 equiv) in THF (10 mL) was added. After 10 minutes, the reaction mixture was warmed to room temperature and stirred for 16 h. After evaporation of the volatiles, the crude residue was dissolved in CH₂Cl₂ (6 mL). The resulting solution was then filtered through Celite and Et₂O (20 mL) was added to the reaction mixture to give a precipitate. The solid was filtered and washed 4 times with Et₂O (10 mL) affording (3)(OTf) as a light-yellow powder (1.38 g, 92%). Single crystals suitable for X-Ray diffraction were grown by layering a solution of (3)(OTf) in CH₂Cl₂ with Et₂O. ¹H NMR (400 MHz, CDCl₃): δ = 7.93 (s, 1H, N₂CH), 7.49 (t, *J* = 1.4 Hz, 1H, CH_{im}), 7.26–7.25 (m, 1H, CH_{im}), 4.18 (sept, *J* = 6.8 Hz, 2H, CH_{IPr}), 3.79 (sept, *J* = 7.0 Hz, 2H, CH_{IPr}), 1.45 (d, *J* = 6.7 Hz, 12H, CH_{3IPr}), 1.26 (d, *J* = 6.8 Hz, 12H, CH_{3IPr}). ¹³C{¹H} NMR (101 MHz, CDCl₃): δ = 137.1 (N₂CH), 131.7 (CH_{im}), 131.4 (C_{Ar}), 120.8 (q, *J* = 322.1 Hz, CF₃SO₃), 119.8 (CH_{im}), 98.9 (C_{Ar}), 57.7 (CH_{IPr}), 48.5 (CH_{IPr}), 21.9 (CH_{3IPr}), 20.8 (CH_{3IPr}). MS (ESI⁺): *m/z* (%): 303.2 (100) [M – OTf]⁺ (calcd 303.2); HRMS (ESI): *m/z*: calcd. for C₁₈H₃₁N₄: 303.2549; found: 303.2553, ϵ_r = 1.3 ppm. Anal. Found, C 48.76, H 7.06, N 11.64. Calcd. for C₁₉H₃₁F₃N₄O₃S.(0.2)CH₂Cl₂: C, 49.12; H, 6.74, N 11.93.

1,3-bis[2,3-bis(diisopropylamino)cyclopropenyl]imidazolium tris-triflate (1·H)(OTf)₃. A solution of (3)(OTf) (863 mg, 1.9 mmol, 1 equiv) in CH₂Cl₂ (8 mL) was stirred at room temperature for 15 minutes for complete dissolution. A solution of (4)(OTf)₂ (1.5 g, 1.9 mmol, 1 equiv) in CH₂Cl₂ (8 mL) was added to the reaction mixture and the resulting solution was stirred for 3 hours. The reaction solution was then concentrated to 3/4 volume and Et₂O (25 mL) was added to the reaction mixture to give a precipitate. The solid was

filtered, washed 4 times with Et₂O (10 mL) and dried under vacuum to give a white powder (1.39 g, 74%). Single crystals suitable for an X-Ray diffraction were grown by layering a solution of (1·H)(OTf)₃ in CH₂Cl₂ with toluene. ¹H NMR (400 MHz, CD₂Cl₂): δ = 10.78 (t, *J* = 1.5 Hz, 1H, N₂CH), 8.85 (d, *J* = 1.5 Hz, 2H, CH_{Im}), 4.18 (sept, *J* = 6.8 Hz, 4H, CH_{IPr}), 3.90 (sept, *J* = 6.7 Hz, 4H, CH_{IPr}), 1.48 (d, *J* = 6.8 Hz, 24H, CH_{IPr}), 1.27 (d, *J* = 6.8 Hz, 24H, CH_{3IPr}). ¹³C{¹H} NMR (101 MHz, CD₂Cl₂): δ = 140.7 (N₂CH), 132.4 (C_{Ar}), 126.9 (CH_{Im}), 120.9 (q, *J* = 321.1 Hz, CF₃SO₃), 91.8 (C_{Ar}), 59.0 (CH_{IPr}), 49.9 (CH_{IPr}), 22.2 (CH_{3IPr}), 20.5 (CH_{3IPr}). MS (ESI⁺): *m/z* (%): 837.4 (100) [M – OTf]⁺ (calcd 837.4); HRMS (ESI): *m/z*: calcd. for C₃₅H₅₉N₆O₆F₆S₂: 837.3842; found: 837.3851, ε_r = 1.1 ppm. Anal. Found, C 43.75, H 6.22, N 8.19. Calcd. for C₃₆H₅₉F₉N₆O₉S₃: C, 43.81; H, 6.03, N 8.51.

1,3-bis[2,3-bis(diisopropylamino)imidazoline-2-selenone bis-triflate (5)(OTf)₂]. Pre-ligand (1·H)(OTf)₃ (100 mg, 0.10 mmol, 1 equiv), K₂CO₃ (20.9 mg, 0.15 mmol, 1.5 equiv) and Se powder (39.8 mg, 0.50 mmol, 5 equiv) were placed in a Schlenk tube. CH₃CN (4 mL) was added and the reaction mixture was stirred at room temperature for 16 h. The reaction mixture was dried under vacuum and the crude residue was dissolved in CH₂Cl₂ (4 mL) and filtered through Celite. The reaction mixture was concentrated to ½ volume and Et₂O (6 mL) was added to get a dark brown precipitate. The solid was filtered, washed 3 times with Et₂O (3 x 2 mL) and dried under vacuum to afford a dark brown crystalline solid (37 mg, 40%). Single crystals suitable for X-Ray diffraction were grown by layering a solution of (5)(OTf)₂ in CH₂Cl₂ with Et₂O. ¹H NMR (600 MHz, CD₃CN): δ = 7.52 (s, 2H, CH_{Im}), 4.13 (sept, *J* = 6.7 Hz, 4H, CH_{IPr}), 3.95 (sept, *J* = 6.7 Hz, 4H, CH_{IPr}), 1.38 (d, *J* = 6.8 Hz, 24H, CH_{IPr}), 1.23 (d, *J* = 6.8 Hz, 24H, CH_{IPr}). ¹³C{¹H} NMR (151 MHz, CD₃CN): δ = 161.6 (N₂C), 133.7 (C_{Ar}), 123.1 (CH_{Im}), 98.1 (C_{Ar}), 59.0 (CH_{IPr}), 49.5 (CH_{IPr}), 22.7 (CH_{3IPr}), 20.7 (CH_{3IPr}). ⁷⁷Se NMR (114.5 MHz, CD₃CN): δ = 196.7. MS (ESI⁺): *m/z* (%): 767.3 (100) [M – OTf]⁺ (calcd 767.3); HRMS (ESI): *m/z*: calcd. for C₃₄H₅₈N₆O₃F₃S⁸⁰Se: 767.3408; found: 767.3417, ε_r = 1.2 ppm

Chloro-(1,5-cyclooctadiene)-[1,3-bis(2,3-bis(diisopropylamino)imidazol-2-ylidene) rhodium(I) bis-triflate (6)(OTf)₂]. Pre-ligand (1·H)(OTf)₃ (100 mg, 0.10 mmol, 1 equiv) and [RhCl(COD)]₂ (24.6 mg, 0.05 mmol, 0.5 equiv) were charged in a Schlenk tube and THF (3 mL) was added to the reaction mixture at –78°C. A solution of KHMDS (0.5 M in toluene, 202 μL, 0.10 mmol, 1 equiv) was added dropwise to the reaction mixture. After 15 minutes, the reaction mixture was warmed to room temperature and stirred for 1 hour. Volatiles were removed under vacuum and the crude residue was dissolved in CH₂Cl₂ (4 mL) and filtered through Celite. The reaction mixture was concentrated to ½ volume and Et₂O (6 mL) was added to give a dark orange precipitate. The precipitate was filtered, washed 3 times with Et₂O (3 x 2 mL) and dried to give (6)(OTf)₂ as a dark orange crystalline solid (74 mg, 70%). ¹H NMR (400 MHz, CD₃CN): δ = 7.63 (s, 2H, CH_{Im}), 5.05 (brs, 2H, CH_{Cod}), 4.33–4.22 (m, 4H, CH_{IPr}), 4.19–4.09 (m, 4H, CH_{IPr}), 3.64–3.54 (brs, 2H,

CH_{Cod}), 2.33–2.24 (m, 4H, CH_{2cod}), 1.71–1.48 (m, 4H, CH_{2cod}), 1.46 (d, *J* = 6.8 Hz, 24H, CH_{3IPr}), 1.37 (d, *J* = 6.8 Hz, 24H, CH_{3IPr}). ¹³C{¹H} NMR (101 MHz, CD₃CN): δ = 190.5 (d, *J*_{RhC} = 53.6 Hz, N₂C), 132.4 (C_{Ar}), 125.6 (CH_{Im}), 122.0 (q, *J* = 321.1 Hz, CF₃SO₃), 103.4 (d, *J*_{RhC} = 6.8 Hz, CH_{Cod}), 101.3 (C_{Ar}), 71.8 (d, *J*_{RhC} = 13.8 Hz, CH_{Cod}), 55.7 (CH_{IPr}), 53.0 (CH_{IPr}), 33.3, 28.8 (CH_{2cod}), 22.5 (CH_{3IPr}), 21.5 (CH_{3IPr}). MS (ESI⁺) *m/z* (%): 897.4 (2) [M – OTf – HCl]⁺ (calcd 897.4), 257.1 (100) [C₂₆H₄₃N₄Rh]²⁺ (calcd 257.1); HRMS (ESI): *m/z*: calcd. for C₄₂H₆₉F₃N₆O₃RhS: 897.4159; found: 897.4169, ε_r = 1.1 ppm.

Chloro-dicarbonyl[1,3-bis(2,3-bis(diisopropylamino)imidazol-2-ylidene)rhodium(I) bis-triflate (7)(OTf)₂]. Complex (6)(OTf)₂ (74 mg, 0.07 mmol, 1 equiv) was dissolved in CD₂Cl₂ (0.7 mL) and CO gas was bubbled into the reaction mixture for 15 minutes at room temperature. NMR of the reaction mixture was immediately recorded showing quantitative formation of (7)(OTf)₂. ¹H NMR (400 MHz, CD₂Cl₂): δ = 8.29 (s, 2H, CH_{Im}), 4.19 (sept, *J* = 6.9 Hz, 4H, CH_{IPr}), 3.97 (sept, *J* = 6.8 Hz, 4H, CH_{IPr}), 1.47 (d, *J* = 6.8 Hz, 24H, CH_{3IPr}), 1.39 (d, *J* = 6.7 Hz, 24H, CH_{3IPr}). ¹³C{¹H} NMR (101 MHz, CD₂Cl₂): δ = 183.5 (d, *J*_{RhC} = 55.0 Hz, Rh-CO), 181.9 (d, *J*_{RhC} = 72.1 Hz, Rh-CO), 181.8 (d, *J*_{RhC} = 45.5 Hz, N₂C), 132.2 (C_{Ar}), 126.2 (CH_{Im}), 121.4 (q, *J* = 322.1 Hz, CF₃SO₃), 99.7 (C_{Ar}), 55.9 (CH_{IPr}), 52.7 (CH_{IPr}), 22.1 (CH_{3IPr}), 20.9 (CH_{3IPr}). IR ν_{CO} (CH₂Cl₂): 2007, 2094 cm⁻¹.

chloro-(η³-allyl)[1,3-bis(2,3-bis(diisopropylamino)imidazole-2-ylidene)palladium(II) bis-triflate (8)(OTf)₂]. Pre-ligand (1·H)(OTf)₃ (100 mg, 0.10 mmol, 1 equiv), [PdCl(allyl)]₂ (18.4 mg, 0.05 mmol, 0.5 equiv) and K₂CO₃ (41.5 mg, 0.30 mmol, 3 equiv) were placed in a Schlenk tube. CH₃CN (4 mL) was added and the reaction mixture was stirred at room temperature for 2 hours. The reaction mixture was dried and the crude residue was dissolved in CH₂Cl₂ (4 mL) and filtered through Celite. The reaction mixture was concentrated to 1/4 volume and Et₂O (4 mL) was added to give a white precipitate. The solid was filtered, washed 3 times with Et₂O (4 x 2 mL) and dried under vacuum to give a white powder (85 mg, 82%). Single crystals suitable for X-Ray diffraction were grown by layering solution of (8)(OTf)₂ in CH₂Cl₂ with Et₂O. ¹H NMR (400 MHz, CD₃CN): δ = 7.82 (s, 2H, CH_{Im}), 5.34 (ddd, *J* = 13.4, 6.6, 4.7 Hz, 1H, CH_{allyl}), 4.24–4.11 (m, 5H, CH_{IPr} + CH_{2allyl}), 4.08–3.87 (m, 4H, CH_{IPr}), 3.59 (dd, *J* = 6.8, 2.3 Hz, 1H, CH_{2allyl}), 3.23 (d, *J* = 13.6 Hz, 1H, CH_{2allyl}), 2.56 (d, *J* = 12.0 Hz, 1H, CH_{2allyl}), 1.40 (d, *J* = 6.8 Hz, 24H, CH_{3IPr}), 1.30 (d, *J* = 6.7 Hz, 12H, CH_{3IPr}), 1.27 (d, *J* = 6.7 Hz, 12H, CH_{3IPr}). ¹³C{¹H} NMR (101 MHz, CD₃CN): δ = 188.0 (N₂C), 132.6 (C_{Ar}), 125.4 (CH_{Im}), 122.0 (q, *J* = 322.1 Hz, CF₃SO₃), 118.1 (CH_{allyl}), 100.2 (C_{Ar}), 74.6 (CH_{2allyl}), 57.6 (CH_{IPr}), 54.8 (CH_{2allyl}), 51.0 (CH_{IPr}), 22.6, 22.5, 21.0, 20.9 (CH_{3IPr}). MS (ESI⁺): *m/z* (%): 869.3 (6) [M – OTf]⁺ (calcd 869.3), 360.2 (76) [M – 2 OTf]²⁺ (calcd 360.2), 225.1 (100) [C₂₁H₃₆N₆Pd]²⁺ (calcd 225.1); HRMS (ESI): *m/z*: calcd. for C₃₇H₆₃N₆O₃F₃PdClS: 869.3368; found: 869.3386, ε_r = 2.1 ppm.

[(η^3 -allyl)] $[\mu$ -1-[2,3-bis(diisopropylamino)cyclopropeno]imidazolyl- κ C²- κ N³]palladium(II)]dimer bis-triflate (9)(OTf)₂. Pre-ligand (1·H)(OTf)₃ (100 mg, 0.10 mmol, 1 equiv), [PdCl(allyl)]₂ (18.4 mg, 0.05 mmol, 0.5 equiv), and K₂CO₃ (41.5 mg, 0.30 mmol, 3 equiv) were placed in a Schlenk tube. CH₃CN (4 mL) was added and the reaction mixture was stirred at room temperature for 48 hours. The reaction mixture was dried and the crude residue was dissolved in CH₂Cl₂ (4 mL) and filtered through Celite. The reaction mixture was concentrated to 1/4 volume and Et₂O (4 mL) was added to get a white precipitate. The solid was then filtered, washed 3 times with Et₂O (4 x 2 mL) and dried under vacuum to give a white powder (46 mg, 75%). Single crystals suitable for X-Ray diffraction were grown by layering a solution of (9)(OTf)₂ in CH₂Cl₂ with Et₂O. ¹H NMR (400 MHz, CD₃CN): δ = 7.24 (brs, 2H, CH_{Im}), 7.13 (s, 1H, CH_{Im}), 7.11 (s, 1H, CH_{Im}), 5.40 (m, 2H, CH_{allyl}), 4.16–4.03 (m, 6H, CH_{iPr} + CH_{2allyl}), 3.93–3.85 (m, 4H, CH_{iPr}), 3.27–3.13 (m, 4H, CH_{2allyl}), 2.28 (m, 2H, CH_{2allyl}), 1.47–1.07 (m, 48H, CH_{3iPr}). ¹³C{¹H} NMR (101 MHz, CD₃CN): δ = 178.1, 177.9 (N₂C), 134.4, 134.2 (CH_{Im}), 132.5 (brs, C_{Ar}), 122.2 (q, J = 322.2 Hz, CF₃SO₃), 120.0, 119.9 (CH_{allyl}), 105.0 (C_{Ar}), 70.2 (CH_{2allyl}), 58.2 (CH_{iPr}), 49.7 (CH_{iPr}), 45.7 (CH_{2allyl}), 22.5, 21.0, 20.9 (CH_{3iPr}). MS (ESI⁺): m/z (%): 1047.3 (1) [M – OTf]⁺ (calcd 1047.3), 450.2 (100) [M – 2 OTf]²⁺ (calcd 450.2); HRMS (ESI): m/z : calcd. for C₄₃H₇₀F₃N₈Pd₂O₃S: 1047.3335; found: 1047.3328, ϵ r = 0.7 ppm.

Chloro-1,3-bis(2,3-bis(diisopropylamino)imidazol-2-ylidene)gold(I) bis-triflate (10)(OTf)₂. Pre-ligand (1·H)(OTf)₃ (200 mg, 0.20 mmol, 1 equiv), AuCl(tht) (64.7 mg, 0.20 mmol, 1 equiv) and K₂CO₃ (83.7 mg, 0.60 mmol, 3 equiv) were placed in Schlenk tube. CH₃CN (6 mL) was added and the reaction mixture was stirred at room temperature for 16 h. The reaction mixture was dried under vacuum and the crude residue was dissolved in CH₂Cl₂ (5 mL) and filtered through Celite. The reaction mixture was concentrated to 1/2 volume and Et₂O (10 mL) was added to get a dark brown precipitate. The solid was filtered, washed 3 times with Et₂O (4 x 2 mL) and dried under vacuum to give a white powder (164 mg, 76%). Single crystals suitable for X-Ray diffraction were grown by layering a solution of (10)(OTf)₂ in CH₂Cl₂ with toluene. ¹H NMR (400 MHz, CD₃CN): δ = 8.00 (s, 2H, CH_{Im}), 4.14 (sept, J = 6.7 Hz, 4H, CH_{iPr}), 3.98 (sept, J = 6.7 Hz, 4H, CH_{iPr}), 1.40 (d, J = 6.7 Hz, 24H, CH_{3iPr}), 1.23 (d, J = 6.7 Hz, 24H, CH_{3iPr}). ¹³C{¹H} NMR (101 MHz, CD₃CN): δ = 176.8 (N₂C), 133.4 (C_{Ar}), 125.8 (CH_{Im}), 122.0 (q, J = 322.1 Hz, CF₃SO₃), 96.9 (C_{Ar}), 59.4 (CH_{iPr}), 49.4 (CH_{iPr}), 22.6 (CH_{3iPr}), 20.5 (CH_{3iPr}). MS (ESI⁺): m/z (%): 919.4 (3) [M – OTf]⁺ (calcd 919.4), 385.2 (100) [M – 2 OTf]²⁺ (calcd 385.2); HRMS (ESI): m/z : calcd. for C₃₄H₅₈N₆O₃F₃SAuCl: 919.3597; found: 919.3604, ϵ r = 0.8 ppm.

Single-crystal X-ray diffraction analyses.

Single crystals suitable for X-ray diffraction were coated with paratone oil and mounted onto the goniometer. The X-ray crystallographic data were obtained at 100K from a Rigaku XtaLAB Synergy diffractometer (Cu K α radiation

source) equipped with an Oxford Cryosystem. The structures have been solved using ShelXT²⁹ and refined by means of least-squares procedures on F using the program CRYSTALS.³⁰ The scattering factors for all the atoms were used as listed in the International Tables for X-ray Crystallography.³¹ Absorption correction was performed using a MULTISCAN procedure.³² All non-hydrogen atoms were refined anisotropically, excepted a triflate anion for (9)(OTf)₂. The H atoms were refined with riding constraints. For (8)(OTf)₂ and (9)(OTf)₂, it was not possible to resolve some diffuse electron-density residuals (enclosed solvent molecules). Some solvent molecules were squeezed with the SQUEEZE facility from PLATON.³³ The structures (1·H)(OTf)₃, (8)(OTf)₂ and (9)(OTf)₂ presented several treated statistic disorders on parts of the ligand or on the allyl groups. For (1·H)(OTf)₃, the crystal was of poor quality with high residual positive density and a disordered triflate anion. For (9)(OTf)₂, one Pd atom was found to be disordered on 2 positions (occupancies 0.75:0.25). However, refinement of the final formulated models leads to imperfect but reasonable solutions. Detailed crystallographic data and structural refinement parameters are given in the SI.

ASSOCIATED CONTENT

Supporting Information

The supporting Information of this article can be found under <https://...>

- ¹H and ¹³C NMR spectra for all new compounds,
- X-ray crystallographic table for compounds (1·H)(OTf)₃, (3)(OTf), (5)(OTf)₂, (8)(OTf)₂, (9)(OTf)₂, and (10)(OTf)₂,
- Catalytic procedures.

AUTHOR INFORMATION

Corresponding Author

* E-mail for V.C.: vincent.cesar@lcc-toulouse.fr

* E-mail for Y.C.: yves.canac@lcc-toulouse.fr

Notes

The authors declare no competing financial interest.

ACKNOWLEDGMENT

The authors thank the Centre National de la Recherche Scientifique for financial support and Alix Saquet for electrochemistry experiments. A. P. is also grateful to the NanoX program for a Master fellowship.

REFERENCES

- (1) (a) Melaimi, M.; Soleilhavoup, M.; Bertrand, G. Stable cyclic carbenes and related species beyond diaminocarbenes. *Angew. Chem. Int. Ed.* **2010**, *49*, 8810–8849. (b) *Top. Organomet. Chem.* Late transition metal complexes of neutral η^1 -carbon ligands: Chauvin, R.; Canac, Y. Eds, Springer, **2010**, *30*, 1–252. (c) Ghadwal, R. S. Carbon-based two electrons σ -donor ligands beyond classical *N*-heterocyclic carbenes. *Dalton Trans.* **2016**, *45*, 16081–16095. (d) Naumann, S. Synthesis, properties & applications of *N*-heterocyclic olefins in catalysis. *Chem. Commun.* **2019**, *55*, 11658–11670. (e) Canac, Y. Carbon ligands: from fundamental aspects to applications. *Molecules* **2021**, *26*, 2132 and references cited herein.
- (2) (a) Baber, R. A.; Clarke, M. L.; Heslop, K. M.; Marr, A. C.; Orpen, A. G.; Pringle, P. G.; Ward, A.; Zambrano-Williams, D. E.

Phenylphosphatrioxa-adamantanes: bulky, robust, electron-poor ligands that give very efficient rhodium(I) hydroformylation catalysts. *Dalton Trans.* **2005**, 1079–1085. (b) Abdellah, I.; Debono, N.; Canac, Y.; Vendier, L.; Chauvin, R. Resolution of the atropochiral biminap ligand and applications in asymmetric catalysis. *Chem. Asian. J.* **2010**, *5*, 1225–12231. (c) Berhal, F.; Esseiva, O.; Martin, C. H.; Tone, H.; Genet, J. P.; Ayad, T.; Ratovelomanana-Vidal, V. (*R*)-3,5-diCF₃-SYNPHOS and (*R*)-*p*-CF₃-SYNPHOS, electron-poor diphosphines for efficient room temperature Rh-catalyzed asymmetric conjugate addition of arylboronic acids. *Org. Lett.* **2011**, *13*, 2806–2809. (d) Anderson, B. G.; Spencer, J. L. The coordination chemistry of pentafluorophenylphosphino pincer ligands to platinum and palladium. *Chem. Eur. J.* **2014**, *20*, 6421–6432. (e) Abe, K.; Kitamura, M.; Fujita, H.; Kunishima, M. Development of highly electron-deficient and less sterically-hindered phosphine ligands possessing 1,3,5-triazinyl groups. *Mol. Catal.* **2018**, *445*, 87–93.

(3) (a) Kuhn, N.; Fahl, J.; Bläser, D.; Boese, R. Synthesis and properties of [Ph₂(Carb)P]AlCl₄ (Carb = 2,3-Dihydro-1,3-disopropyl-4,5-dimethylimidazol-2-ylidene) – a stable carbene complex of trivalent phosphorus. *Z. Anorg. Allg. Chem.* **1999**, *625*, 729–734. (b) Petuskova, J.; Bruns, H.; Alcarazo, M. Cyclopropenylidene-stabilized diaryl and dialkyl phosphonium cations: Applications in homogeneous gold catalysis. *Angew. Chem. Int. Ed.* **2011**, *50*, 3799–3802. For review articles, see; (c) Canac, Y.; Maaliki, C.; Abdellah, I.; Chauvin, R. Carbeniophosphanes and their carbon > phosphorus → metal ternary complexes. *New J. Chem.* **2012**, *36*, 17–27. (d) Alcarazo, M. Synthesis, Structure, and Applications of α -Cationic Phosphines. *Acc. Chem. Res.* **2016**, *49*, 1797–1805. (e) Canac, Y. Carbeniophosphines versus phosphoniocarbenes: the role of the positive charge. *Chem. Asian. J.* **2018**, *13*, 1872–1887. (f) Rugen, C. J.; Alcarazo, M. α -Cationic phosphines: from curiosities to powerful ancillary ligands. *Synlett* **2022**, *33*, 16–26.

(4) (a) Azouri, M.; Andrieu, J.; Picquet, M.; Catey, H. Synthesis of new cationic donor-stabilized phosphonium adducts and their unexpected P-substituent exchange reactions. *Inorg. Chem.* **2009**, *48*, 1236–1242. (b) Weigand, J. J.; Feldmann, K. O.; Henne, F. D. Carbene-stabilized phosphorus(III)-centered cations [LPX₂]⁺ and [L₂PX]²⁺ (L = NHC; X = Cl, CN, N₃). *J. Am. Chem. Soc.* **2010**, *132*, 16321–16323. (c) Feldmann, K. O.; Weigand, J. J. Multiple-charged P₁-centered cations: Perspectives in synthesis. *Angew. Chem. Int. Ed.* **2012**, *51*, 6566–6568. (d) Maaliki, C.; Lepetit, C.; Canac, Y.; Bijani, C.; Duhayon, C.; Chauvin, R. On the P-coordinating limit of NHC-phosphonium cations towards Rh⁺ centers. *Chem. Eur. J.* **2012**, *18*, 7705–7714. (e) Maaliki, C.; Canac, Y.; Lepetit, C.; Duhayon, C.; Chauvin, R. P-oxidation of gem-dicationic phosphines. *RSC Adv.* **2013**, *3*, 20391–20398. (f) Henne, F. D.; Dickschat, A. T.; Hennersdorf, F.; Feldmann, K. O.; Weigand, J. J. Synthesis of selected cationic pnictanes [L_nPnX_{3-n}]ⁿ⁺ (L = Imidazolium-2-yl; Pn = P, As; n = 1–3) and replacement reactions with pseudohalogens. *Inorg. Chem.* **2015**, *54*, 6849–6861.

(5) (a) Carreras, J.; Gopakumar, G.; Gu, L.; Gimeno, A.; Linowski, P.; Petuskova, J.; Thiel, W.; Alcarazo, M. Polycationic ligands in gold catalysis: synthesis and applications of extremely π -acidic catalysts. *J. Am. Chem. Soc.* **2013**, *135*, 18815–18823. (b) Mehler, G.; Linowski, P.; Carreras, J.; Zanardi, A.; Dube, J. W.; Alcarazo, M. Bis(cyclopropenium)phosphines: synthesis, reactivity, and applications. *Chem. Eur. J.* **2016**, *22*, 15320–15327. (c) Mboyi, C. D.; Maakili, C.; Mankou Makaya, A.; Canac, Y.; Duhayon, C.; Chauvin, R. Phosphonium versus pro-phosphide character of P-*tert*-butyl-dicyclopropenylphosphine: zwitterionic palladate complexes of a dicationic phosphido ligand. *Inorg. Chem.* **2016**, *55*, 11018–11027.

(6) (a) Bourissou, D.; Guerret, O.; Gabbai, F. P.; Bertrand, G. Stable carbenes. *Chem. Rev.* **2000**, *100*, 39–91. (b) Hopkinson, M. N.; Richter, C.; Schedler, M.; Glorius, F. An overview of N-heterocyclic carbenes. *Nature* **2014**, *510*, 485–496. (c) Vivercos, A.; Segarra, C.; Albrecht, M. Mesoionic and related less heteroatom-stabilized N-heterocyclic carbene complexes: synthesis, catalysis, and other applications. *Chem. Rev.* **2018**, *118*, 9493–9586. (d) Smith, C. A.; Narouz, M. R.; Lummis, P. A.; Singh, I.; Nazemi, A.; Li, C.-H.; Crudden, C. M. N-Heterocyclic Carbenes in Materials Chemistry. *Chem. Rev.* **2019**, *119*, 4986–5056. (e) Sau, S. C.; Hota, P. K.; Mandal, S. K.; Soleilhavoup, M.; Bertrand, G. Stable abnormal N-heterocyclic carbenes and their applications. *Chem. Soc. Rev.* **2020**, *49*, 1233–1252. (f) Zhao, Q.; Meng, G.; Nolan,

S. P.; Szostak, M. N-Heterocyclic Carbene Complexes in C–H Activation Reactions. *Chem. Rev.* **2020**, *120*, 1981–2048.

(7) NHCs bearing a negative charge have been also reported. For a review, see: (a) Nasr, A.; Winkler, A.; Tamm, M. Anionic N-heterocyclic carbenes: Synthesis, coordination chemistry and applications in homogeneous catalysis. *Coord. Chem. Rev.* **2016**, *316*, 68–124. For key examples, see: (a) César, V.; Lugan, N.; Lavigne, G. A stable anionic N-Heterocyclic carbene and its zwitterionic complexes. *J. Am. Chem. Soc.* **2008**, *130*, 11286–11287. (b) Kronig, S.; Theuergarten, E.; Daniliuc, C. G.; Jones, P. G.; Tamm, M. Anionic N-Heterocyclic carbenes that contain a weakly coordinating borate moiety. *Angew. Chem. Int. Ed.* **2012**, *51*, 3240–3244. (c) El-Hellani, A.; Lavallo, V. Fusing N-Heterocyclic carbenes with carborane anions. *Angew. Chem. Int. Ed.* **2014**, *53*, 4489–4493. (d) César, V., Mallardo, V., Nano, A., Dahm, G., Lugan, N., Lavigne, G., Bellemin-Lapondaz, S. IMes-acac: hybrid combination of diaminocarbene and acetylacetonato sub-units into a new anionic ambidentate NHC ligand. *Chem. Commun.* **2015**, *51*, 5271–5274.

(8) (a) Buhl, H.; Ganter, C. Tuning the electronic properties of an N-heterocyclic carbene by charge and mesomeric effects. *Chem. Commun.* **2013**, *49*, 5417–5419. (b) Hölzel, T.; Otto, M.; Buhl, H.; Ganter, C. An extremely electron poor cationic triazoliumylidene N-Heterocyclic carbene: experimental and computational studies. *Organometallics*, **2017**, *36*, 4443–4450. (c) Regnier, V.; Planet, Y.; Moore, C. E.; Pecaut, J.; Philouze, C.; Martin, D. Stable di- and tri-coordinated carbon(II) supported by an electron-rich β -diketiminato ligand. *Angew. Chem. Int. Ed.* **2017**, *56*, 1031–1035. (d) Iglesias-Sigüenza, J.; Izquierdo, C.; Díez, E.; Fernández, R.; Lassaletta, J. M. N-Heterocyclic cationic carbene ligands. Synthesis, reactivity and coordination chemistry. *Dalton Trans.* **2018**, *47*, 5196–5206. (e) Appel, S.; Brüggemann, P.; Ganter, C. A tropylium annulated N-heterocyclic carbene. *Chem. Commun.* **2020**, *56*, 9020–9023.

(9) (a) Schwedtmann, K.; Schoemaker, R.; Hennersdorf, F.; Bauzá, A.; Frontera, A.; Weiss, R.; Weigand, J. J. Cationic 5-phosphonio-substituted N-heterocyclic carbenes. *Dalton Trans.* **2016**, *45*, 11384–11396. (b) Ruamps, M.; Lugan, N.; César, V. A cationic N-Heterocyclic carbene containing an ammonium moiety. *Organometallics*, **2017**, *36*, 1049–1055.

(10) (a) Vanicek, S.; Podewitz, M.; Stubbe, J.; Schulze, D.; Kopacka, H.; Wurst, K.; Müller, T.; Lippmann, P.; Haslinger, S.; Schottenberger, H.; Liedl, K. R.; Ott, I.; Sarkar, B.; Bildstein, B. Highly electrophilic, catalytically active and redox-responsive cobaltoceniumyl and ferrocenyl triazolylidene coinage metal complexes. *Chem. Eur. J.* **2018**, *24*, 3742–3753. (b) Vanicek, S.; Beerhues, J.; Bens, T.; Levchenko, V.; Wurst, K.; Bildstein, B.; Tilset, M.; Sarkar, B. Oxidative access via aqua regia to an electrophilic, mesoionic dicobaltoceniumyltriazolylidene gold(III) catalyst. *Organometallics* **2019**, *38*, 4383–4386. (c) Tarrieu, R.; Delgado, I. H.; Zinna, F.; Dorcet, V.; Colombel-Rouen, S.; Crévisy, C.; Baslé, O.; Bosson, J.; Lacour, J. Hybrids of cationic [4]helicene and N-heterocyclic carbene as ligands for complexes exhibiting (chir) optical properties in the far red spectral window. *Chem. Commun.* **2021**, *57*, 3793–3796. (d) Malchou, C.; Fries, D. V.; Mees, Y.; Jakobs, M. F.; Sun, Y.; Becker, S.; Niedner-Schatteburg, G.; Thiel, W. R. Transition metal complexes of NHC ligands functionalized with the cationic (η^5 -cyclopentadienyl)(η^6 -phenyl) iron(II) motif. *Eur. J. Inorg. Chem.* **2022**, *16*, 1–9.

(11) Barthes, C.; Duhayon, C.; Canac, Y.; César, V. N-Cyclopropenyl-imidazol-2-ylidene: An N-heterocyclic carbene bearing an N-cationic substituent. *Chem. Commun.* **2020**, *56*, 3305–3308.

(12) Dube, J. W.; Zheng, Y.; Thiel, W.; Alcarazo, M. α -Cationic arsines: synthesis, structure, reactivity, and applications. *J. Am. Chem. Soc.* **2016**, *138*, 6869–6877.

(13) (a) Weiss, R.; Engel, S. Poly-onio substituted phosphorus compounds. *Synthesis*, **1991**, *12*, 1077–1079. (b) Conejero, S.; Canac, Y.; Tham, F. S.; Bertrand, G. Readily available onio-substituted methyleneiminium salts: single precursors for a variety of aminocarbenes. *Angew. Chem. Int. Ed.* **2004**, *43*, 4089–4093.

(14) Kozma, Á.; Petuskova, J.; Lehmann, C. W.; Alcarazo, M. Synthesis, structure and reactivity of cyclopropenyl-1-ylidene stabilized S(II), Se(II) and Te(II) mono- and dications. *Chem. Commun.* **2013**, *49*, 4145–4147.

- (15) CCDC 2191626–2191631 contain full crystallographic information for compounds (1·H)(OTf)₃, (3)(OTf), (5)(OTf)₂, (8)(OTf)₂, (9)(OTf)₂, and (10)(OTf)₂. These data can be obtained free of charge from the Cambridge Crystallographic Data Centre via www.ccdc.cam.ac.uk/data_request/cif.
- (16) ¹³C NMR carbenic resonance of 1²⁺ ($\delta_{\text{C}} = 221.0$ ppm) was observed at -78°C by adding one equiv. of KHMDS in THF-*d*⁸ to (1·H)(OTf)₃. However, this NHC was found to be unstable, decomposing at temperatures above -40°C into an unidentified mixture of products.
- (17) Verlinden, K.; Buhl, H.; Frank, W.; Ganter, C. Determining the Ligand Properties of N-Heterocyclic Carbenes from ⁷⁷Se NMR Parameters. *Eur. J. Inorg. Chem.* **2015**, *2015*, 2416–2425.
- (18) Urbina-Blanco, C. A.; Bantreil, X.; Clavier, H.; Slawin, A. M. Z.; Nolan, S. P. Backbone tuning in indenylidene–ruthenium complexes bearing an unsaturated N-heterocyclic carbene. *Beilstein J. Org. Chem.* **2010**, *6*, 1120–1126.
- (19) Buhl, H., Verlinden, K., Ganter, C., Novaković, S. B., Bogdanović, G. A. Electrostatic properties of N-Heterocyclic carbenes obtained by experimental charge-density analysis of two selenium adducts. *Eur. J. Inorg. Chem.* **2016**, *2016*, 3389–3395.
- (20) Martynova, E. A.; Tzouras, N. V.; Pisanò, G.; Cazin, C. S. J.; Nolan, S. P. The “weak base route” leading to transition metal–N-heterocyclic carbene complexes. *Chem. Commun.* **2021**, *57*, 3836–3856.
- (21) (a) Huynh, H. V. Electronic Properties of N-Heterocyclic Carbenes and Their Experimental Determination. *Chem. Rev.* **2018**, *118*, 9457–9492. (b) Nelson, D. J.; Nolan, S. P. Quantifying and understanding the electronic properties of N-heterocyclic carbenes. *Chem. Soc. Rev.* **2013**, *42*, 6723–6753.
- (22) Based on calculated TEP value (2108.7 cm⁻¹), dicationic triazolylidene featuring two cobaltoceniumyl substituents was reported to be an extremely electron-poor NHC (see ref.10a).
- (23) (a) Hering, F.; Radius, U. From NHC to imidazolyl ligand: synthesis of platinum and palladium complexes d¹⁰-[M(NHC)₂] (M = Pd, Pt) of the NHC 1,3-diisopropylimidazolin-2-ylidene. *Organometallics* **2015**, *34*, 3236–3245. (b) Martinez, E. E.; Jensen, C. A.; Larson, A. J. S.; Kenney, K. C.; Clark, K. J.; Hadi Nazari, S.; Valdivia-Berroeta, G. A.; Smith, S. J.; Ess, D. H.; Michaelis, D. J. Monosubstituted, anionic imidazolyl ligands from N–H NHC precursors and their activity in Pd-catalyzed cross-coupling reactions. *Adv. Synth. Catal.* **2020**, *362*, 2876–2881.
- (24) (a) Abdellah, I.; Lepetit, C.; Canac, Y.; Duhayon, C.; Chauvin, R. Imidazolophosphines are true N-Heterocyclic carbene (NHC)-phosphenium adducts. *Chem. Eur. J.* **2010**, *16*, 13095–13108. (b) Abdellah, I.; Boggio-Pasqua, M.; Canac, Y.; Lepetit, C.; Duhayon, C.; Chauvin, R. Towards the limit of atropochiral stability: H-Miop, an N-heterocyclic carbene precursor and cationic analogue of the H-MOP ligand. *Chem. Eur. J.* **2011**, *17*, 5110–5115.
- (25) Falivene, L.; Cao, Z.; Petta, A.; Serra, L.; Poater, A.; Oliva, R.; Scarano, V.; Cavallo, L. Towards the online computer-aided design of catalytic pockets. *Nature Chem.* **2019**, *11*, 872–879.
- (26) Brüggemann, P.; Wahl, M.; Schwengers, S.; Buhl, H.; Ganter, C. Access to a cationic, electron-poor N-Heterocyclic carbene with a quinazolinium core by postsynthetic modification of related neutral derivatives. *Organometallics*, **2018**, *37*, 4276–4286.
- (27) Marion, N.; Navarro, O.; Mei, J.; Stevens, E. D.; Scott, N. M.; Nolan, S. P. Modified (NHC)Pd(allyl)Cl (NHC = N-Heterocyclic carbene) complexes for room-temperature Suzuki–Miyaura and Buchwald–Hartwig reactions. *J. Am. Chem. Soc.* **2006**, *128*, 4101–4111.
- (28) Hashmi, A. S. K.; Hengst, T.; Lothschütz, C.; Rominger, F. New and easily accessible nitrogen acyclic gold(I) carbenes: structure and application in the gold-catalyzed phenol synthesis as well as the hydration of alkynes. *Adv. Synth. Catal.* **2010**, *352*, 1315–1337.
- (29) Sheldrick, G. M. SHELXT - Integrated space-group and crystal-structure determination, *Acta Cryst.* **2015**, *A71*, 3–8.
- (30) Betteridge, P. W.; Carruthers, J. R.; Cooper, R. I.; Prout, K.; Watkin, D. J. CRYSTALS version 12: software for guided crystal structure analysis. *J. Appl. Cryst.* **2003**, *36*, 1487.
- (31) Sheldrick, G. M. A short history of SHELX. *Acta Cryst.* **2008**, *A64*, 112–122.
- (32) Blessing, R. H. An empirical correction for absorption anisotropy. *Acta Cryst.* **1995**, *A51*, 33–38.
- (33) Spek, A. L. PLATON SQUEEZE: a tool for the calculation of the disordered solvent contribution to the calculated structure factors. *Acta Cryst. Sect. C*, **2015**, *71*, 9–18.

Table of Contents Only

